
Article:
Tsakiropoulos, P. orcid.org/0000-0001-7548-3287 (2017) On the Nb silicide based alloys: Part I – The bcc Nb solid solution. Journal of Alloys and Compounds. ISSN 0925-8388

https://doi.org/10.1016/j.jallcom.2017.03.070

Accepted Manuscript

On the Nb silicide based alloys: Part I – The bcc Nb solid solution

P. Tsakiropoulos

PII: S0925-8388(17)30839-3

DOI: 10.1016/j.jallcom.2017.03.070

Reference: JALCOM 41108

To appear in: *Journal of Alloys and Compounds*

Received Date: 6 July 2016

Revised Date: 31 January 2017

Accepted Date: 6 March 2017

Please cite this article as: P. Tsakiropoulos, On the Nb silicide based alloys: Part I – The bcc Nb solid solution, *Journal of Alloys and Compounds* (2017), doi: 10.1016/j.jallcom.2017.03.070.

On the Nb silicide based alloys: Part I – The bcc Nb solid solution

P Tsakiropoulos*

Department of Materials Science and Engineering,

The University of Sheffield, Sheffield S1 3JD, UK

Abstract

This paper is about the three types of bcc Nb_{ss} solid solution, namely normal Nb_{ss}, Nb_{ss} rich in Ti and Nb_{ss} with no Si that are observed in multi-component Nb silicide based alloys of Nb-Si-TM-RM-X (TM = Cr, Hf, Ti, V, RM = Mo, Ta, W, X = Al, B, Ge, Sn) systems. The entropy (ΔS_{mix}) and enthalpy (ΔH_{mix}) of mixing, atomic size difference (δ), electronegativity difference ($\Delta\chi$), valence electron concentration (VEC) and the parameter $Q = T_m \Delta S_{mix} /|\Delta H_{mix}|$ were calculated for fifty four solid solutions. The values of these parameters were $-2 < \Delta H_{mix} < -15.9$ kJ/mol, $5.8 < \Delta S_{mix} < 14.5$ J/molK, $2.4 < \delta < 9.7$, $4.4 < VEC < 5.4$, $0.039 < \Delta\chi < 0.13$ and $0.179 < \Delta\chi < 0.0331$ and $1.55 < Q < 8.9$. The solid solutions with $\Delta\chi > 0.179$ had no B, Ta and V and the solid solutions with no W had $\Delta\chi < 0.13$. The atomic size difference parameter δ could separate the Nb_{ss} rich in Ti ($\delta > 5$) and the Nb_{ss} with no Si ($\delta < 5$). The formation of Ti rich Nb_{ss} and Nb_{ss} with no Si was attributed to the partitioning of Mo, Ti and W.

Keywords: A – High temperature alloys, Solid solution

*p.tsakiropoulos@sheffield.ac.uk, fax: +44 114 222 5943

Introduction

Future environmental and performance targets for aero-engines can be met with propulsive and thermal efficiency changes and the availability of new materials with capabilities beyond those of Ni based superalloys. Niobium silicide based alloys (also known as Nb *in situ* composites) have the potential to offer balance of properties required in critical applications in future aero-engines [1]. These materials are multicomponent alloys with microstructures consisting of solid solution(s) and intermetallic(s) phases.

Multicomponent Nb silicide based alloys with transition metals (Cr, Fe, Hf, Ti, V, Zr) [2 - 4], refractory metals (Mo, Ta, W) [4, 5] and simple metal and metalloid (Al, B, Ge, Sn) [6 - 10] additions can meet either one or two of the property goals [1] and alloys with the aforementioned alloying additions can offer a balance of room, intermediate and high temperature properties including oxidation resistance. The latest generation of developmental alloys can have 12 solute additions to Nb.

Compared with ferrous alloys, light metal (Al, Mg, Ti) alloys and Ni based superalloys the design of Nb silicide based alloys is hindered by the lack of data. Experimental data about thermodynamic properties of Nb based systems are limited [11, 12]. Phase equilibria data are available for a small number of systems from thermodynamic modelling (CALPHAD) and *ab initio* calculations. For the Nb-Si binary, which is the basis for developing the Nb silicide based alloys, there is disagreement regarding the temperature ranges where the Nb_3Si and Nb_5Si_3 silicides are stable and the composition of the eutectic $L \rightarrow Nb_{ss} + Nb_3Si$ [13 - 16], in some calculated phase diagrams the Nb_5Si_3 is considered as a single phase [16] and in others as two phases (βNb_5Si_3 and αNb_5Si_3, see below) [13, 17], and most calculations do not account for the solubility range of αNb_5Si_3 [18, 19]. There are also disagreements between ternary phase diagrams of the same system. For example, for the Nb-Cr-Si system (Cr is an important addition regarding its effects on the oxidation and toughness of Nb silicide based alloys) there is disagreement about the phase equilibria between Nb_{ss}, Nb_5Si_3 and $NbCr_2$ and the liquidus projection [20 -23]. For the Nb-Ti-Si system (Ti is important alloying element in Nb silicide based alloys for achieving a balance of properties) there is disagreement for the liquidus projection [16, 24, 25] and in particular the αNb_5Si_3 [24, 25]. Furthermore, *ab initio* calculations do not agree with results of the thermodynamic modelling of the stability of $(Nb,Ti)_5Si_3$, i.e., how the substitution of Nb by Ti in Nb_5Si_3 affects the stability of the latter [26]. There are also conflicting reports for the Nb-Ge binary [27], which is an important system for the development of Nb silicide based alloys because alloying with Ge improves their oxidation resistance [28].

Binary phase diagrams of refractory metals exist only for high temperatures ($T > 2273$ K). In the refractory metal binaries of interest to Nb silicide based alloys, namely Nb-Mo, Nb-Ta, Nb-W (Mo, Ta and W provide solid solution strengthening and improve the high temperature strength and creep of Nb silicide based alloys), a single A2 phase exists across the entire composition. Experimental data for thermodynamic properties (if available) is likely not to be accurate for these systems. In the majority of phase diagrams phase equilibria below 273 K is not available.

In Nb silicide based alloys the most important phases are the bcc Nb solid solution (Nb_{ss}) and the Nb_5Si_3 silicide. The former can form in three types, namely normal Nb_{ss}, Nb_{ss} rich in Ti and Nb_{ss} with no Si [4, 5, 29]. The Nb_{ss} with no Si is rich in Mo and W. The 5-3 silicide can

form with tetragonal (βNb_5Si_3 – tP32, W_5Si_3, $D8_m$ and αNb_5Si_3 – tP32, Cr_5B_3, $D8_l$) or hexagonal (γNb_5Si_3 – hP16, Mn_5Si_3, $D8_8$) structure. Other intermetallics such as Nb_3Si, Laves and A15 phases can also be present [1 - 10, 22, 29]. The unalloyed tetragonal Nb_5Si_3 and Nb respectively have poor room temperature fracture toughness (about 3 MPa$\sqrt{m}$) [30] and high creep exponent (≈ 6, the creep exponent of Nb_5Si_3 is about 1 [31]). Niobium has poor oxidation behaviour.

The fracture related properties, creep and oxidation behaviour of a Nb silicide based alloy critically depend on the chemistry, volume fraction and distribution of the Nb_{ss} in its microstructure as well as on the properties of the intermetallic(s) that are present in it. A high volume fraction of Nb_{ss} is good for toughness but not for oxidation and creep. Solid solution strengthened Nb_{ss} is desirable for high temperature strength and creep but not all additions that can provide solid solution strengthening will improve oxidation and toughness. The solid solubility of specific solutes in the Nb_{ss} depends on the solubility of other elements [29], and is crucial for toughness [30, 31]. The diffusivity of oxygen critically depends on the solute elements and their concentrations in the alloy [32].

The prediction of solid solubility in binary alloys was studied by Hume-Rothery and co-workers [33, 34], Darken and Gurry [35], Cschneidner [36], Waber et al [37], Chelikowsky [38], Alonso and co-workers [39, 40], and has been discussed in [41] and reviewed by Massalski [42], Cottrell [43], Pettifor [44], and Cschneidner and Verkade [45] and many other researchers. Criteria ("rules") based on atomic size, electronegativity, valence, electron density at the boundary of the Wigner-Seitz cell [38 - 40] have been proposed and the phenomenological approach developed by Miedema and his collaborators [46 - 48] has been used to predict solid solubilities in binary systems. The above predictive methods defined a concentration criterion (not always the same) for the solubility of an element, determined boundary/ies for soluble elements in a host element and presented the soluble elements in a host element using Darken-Gurry maps [35] and Chelikowsky plots [38]. The above, which are also known as classical methods for predicting solid solubility, are enthalpy (bonding) based, do not consider the entropic term, are effective in the Henrian solubility range and have been used to predict solubilities in binary systems, for example in uranium based binary systems [49].

Engineering alloys are rarely binary alloys. Latest generation Ni based superalloys can have as many as 12 solute additions and in these alloys the same number of elements can be present as solutes in the fcc Ni solid solution (γ-Ni_{ss}). The γ-Ni_{ss} in these alloys can be predicted using CALPHAD, which can also give the solid solubilities of solute additions. This prediction is possible because for this family of alloys (i.e., the Ni based superalloys) thermodynamic databases are available. Predictions using such databases are thought to be reliable when the considered alloy falls in the composition range over which the database was constructed. For alloys falling outside the compositions used to construct the database, predictions could be less reliable and should be considered with caution. The aforementioned classical methods [33 – 44] cannot predict multi-element solid solutions and the solid solubilities of each of the different solute elements.

Recently, the prediction of the formation of solid solution(s) and/or intermetallic(s) in multicomponent alloys has been addressed in research on equiatomic or near equiatomic (or with percentage of each element between 5 and 35 at%) multi-element ($\geq$5) solid solution or solid solution + intermetallic(s) alloys that are referred to as multi-component

alloys (MCA), or “high entropy alloys” (HEA) or multi-principle element alloys (MPEA) or complex concentrated alloys (CCA) in the literature [50, 51, 52]. Few such alloys are now known to be single phase solid solution alloys (meaning the stability of single phase solid solution at elevated temperatures has been validated), most are multiphase alloys. Examples are the bcc NbMoTaVW and NbHfTiTaZr solid solution alloys [50, 53] and the alloy AlCoCrCuFeNi with solid solution + intermetallics stable phases in its microstructure [54].

Prediction of stable phases in an alloy is not always possible using CALPHAD owing to the lack of reliable databases. Single phase solid solution alloys can be predicted by CALPHAD when extensive solid solutions exist in all edge binaries and ternary systems [e.g., 55]. For selecting an HEA (or MCA, MPEA, CCA) alloy the alternatives to CALPHAD have been to use *ab initio* calculations or combine the latter with CALPHAD or use approaches (inspired from guidelines devised originally for glassy alloys) that combine empirical rules from the aforementioned research on solid solubility in binary alloys [33 – 41] with data from the Miedema model [56] and thermodynamics. An example of the former is the use of *ab initio* molecular dynamics simulations [57] to predict the NbHfTiTaZr and $Al_{1.3}$CoCrCuFeNi alloys as solid solution and solid solution + intermetallic(s) alloys, respectively. These calculations also showed that the single solid solution NbHfTiTaZr formed because for this composition there is no short-range order and segregation in the liquid. An example of the latter is an approach that was initially adopted for single phase solid solution HEA and uses empirical rules based on atomic size, electronegativity, valence electron concentration, and enthalpies and entropies of mixing $\Delta S_{mix} = \Delta S_{conf} = - R \Sigma^{n}_{i=1} [x_i \ln x_i]$ (ideal and regular solutions) and $\Delta H_{mix} = \Sigma^{n}_{i=1,i\neq j} [\Omega_{ij} x_i x_j]$ where R is the gas constant, x_i and x_j are the fractions of components i and j, respectively and the parameter Ω_{ij} is from data from Miedema’s model for liquid alloys or from experimental mixing enthalpies of i-j binaries (if available) [58]. In this approach the implicit assumption is made that entropic contributions from electronic and magnetic excitations and atomic vibrations can be neglected in determining which phases will be stable. The regular solution model does not take into account short range order in alloys, considers only the energy of pair atomic interactions, is applicable to systems with very similar size components and rarely is applicable to real alloys [59]. Weak dependence of single phase solid solution formability on configurational entropy has been demonstrated [52].

Phase selection among different phases is determined by the Gibbs free energy of all competing phases. The Gibbs free energy change includes enthalpy and entropy contributions and other terms such as strain energy. The equilibrium state represents the minimum energy state of the system and can be a mixture of solid solution(s) and intermetallic(s), or solid solution(s) or intermetallic(s). The free energy change for solid solution is $\Delta G_{ss} = \Delta H_{mix} - T\Delta S_{mix}$ and for intermetallic $\Delta G_{IM} = \Delta H_f - T\Delta S_f$, where ΔH_f and ΔS_f are the formation enthalpy and entropy of intermetallic. The enthalpy of mixing, which is commonly negative in alloys, with the configurational entropy increase the stability of disordered solid solution phases. For ordered intermetallic phases the ΔS_f is small compared with the ΔH_f. Thus, ΔH_{mix} and ΔS_{mix} stabilise disordered solid solutions and ΔH_f destabilises them [51].

The enthalpies and entropies of mixing of solid solutions and ΔH_f for intermetallic phases in alloys of systems for which there is reliable thermodynamic data can be calculated using CALPHAD. Some experimental ΔH_f data is available for unalloyed intermetallics. For

unalloyed (e.g. Nb_5Si_3) and simply alloyed (e.g. $(Nb,Ti)_5Si_3$) intermetallics ΔH_f data can be generated from *ab initio* calculations [27, 28, 60, 61] but for highly alloyed intermetallics in multicomponent alloys such calculations are complicated and not trivial. For example, Nb silicide based alloys can have as many as 12 solute additions, and in the stable 5-3 silicide phase the Nb can be substituted by 8 transition and refractory metals and Si by 4 simple metals and metalloids. Estimates of ΔH_f must be made for all possible crystal structures for given atoms and stoichiometries to find the most negative ΔH_f value. In the same alloy the stable solid solution could have 12 solutes. In a similar alloy with the same solute additions but with different concentrations the stable solid solution could be with 11 solutes and no Si.

Phenomenological and empirical models using the enthalpy and entropy of mixing and parameters from the classical methods [33-44], such as the atomic size, electronegativity etc. are employed to predict the formation of solid solution(s) and/or intermetallic(s) or amorphous phases [58, 62 - 64] and HEAs [65] because for multicomponent alloys the full range of enthalpy and entropy values for different phases are not readily accessible via CALPHAD and/or ab initio calculations. The models and experimental results have shown that the entropy of mixing is not an effective phase selection parameter compared with the enthalpy of mixing and atomic size mismatch [52, 65].

The Nb_{ss} can be the Achilles' heel of Nb silicide based alloys because its properties, volume fraction and distribution in the microstructure are crucial for achieving a balance of room, intermediate and elevated temperature properties in the alloys. This paper concentrates on the types of Nb_{ss} that can form in Nb silicide based alloy. The motivation for the research presented in this paper was to find out the ranges of the parameters that phenomenological and empirical models use to describe solid solutions. In the companion paper (Part II [66]) the same parameters are used to study the alloys in which the solid solutions were formed.

Method of Analysis of Data

The fifty four Nb solid solutions studied in this paper (Table 1) were in the cast (AC) and heat treated (HT) microstructures of alloys of Nb-Si-TM-RM-X (TM = Cr, Hf, Ti, V, RM = Mo, Ta, W, X = Al, B, Ge, Sn) systems. The alloys were studied previously, meaning no new alloys were prepared for this study and no solid solutions were analysed in this study. Alloy compositions can be found in [2 – 4, 6, 8 – 10, 29, 67 - 70]. In the previous research the microstructures were studied using scanning electron microscopy (SEM), electron probe microanalysis (EPMA) and X-ray diffraction. The bcc crystal structure of the Nb_{ss} was confirmed by XRD and the chemical composition of the Nb_{ss} solid solutions was determined using EPMA [2 – 4, 6, 8 – 10, 29, 67 - 70]. In rare occasions precipitation of second phase [71] is observed in the Nb_{ss} of some Nb silicide based alloys. The solid solutions of such alloys were not included in this study.

The chemical analysis (EPMA) data for each Nb_{ss} solid solution was used to calculate the atomic size difference (δ), electronegativity difference ($\Delta\chi$), valence electron concentration (VEC), entropy (ΔS_{mix}) and enthalpy (ΔH_{mix}) of mixing and $Q = T_m \Delta S_{mix} / |\Delta H_{mix}|$ using the following equations

$$\delta = 100\sqrt{\sum_{i=1}^{n} c_i(1-r_i/\bar{r})^2} \quad (1)$$

$$\Delta H_{\text{mix}} = \sum_{i=1, i\neq j}^{n} \Omega_{ij} c_i c_j \quad (2)$$

$$\Delta S_{\text{mix}} = -R\sum_{i=1}^{n} c_i \ln c_i \quad (3)$$

$$\Delta\chi = \sqrt{\sum_{i=1}^{n} c_i(\chi_i - \bar{\chi})^2} \quad (4)$$

$$\text{VEC} = \sum_{i=1}^{n} c_i (\text{VEC})_i \quad (5)$$

where

$$\bar{r} = \sum_{i=1}^{n} c_i r_i$$

$$\Omega_{ij} = 4\Delta_{\text{mix}}^{AB}$$

$$\bar{\chi} = \sum_{i=1}^{n} c_i \chi_i$$

and c_i and r_i respectively are the concentration in at% and the atomic radius of the ith element [64] (the factor 100 is used to amplify the data), Δ_{AB}^{mix} is the enthalpy of mixing of binary A-B alloy (data from [72]), R is the gas constant, and χ_i and $(VEC)_i$ is the Pauling electronegativity and the VEC [73] of the ith element (data for χ_i and $(VEC)_i$ from [64]).

Phase stability can be considered in terms of *e/a* (an averaged valency of alloying elements in an alloy) and VEC (number of valence electrons per atom filled into the valence band). The former is the parameter in the Hume-Rothery rules [34] and the latter is key to determining the Fermi level in the valence band. The choice between *e/a* and VEC depends on the stability mechanism involved [73]. According to Mizutani and co-workers [73, 74] the *e/a* is difficult to use as a universal parameter in alloy design because its value cannot be

uniquely assigned to a transition metal owing to its dependence on the surrounding environment. Instead, VEC is a more important parameter in transition metal alloys [73, 74].

Results and Discussion

The VEC, δ, $\Delta\chi$, T_m (K), ΔH_{mix} ($kJmol^{-1}$), ΔS_{mix} ($Jmol^{-1}K^{-1}$), and Q values for different bcc Nb_{ss} solid solutions formed in different Nb silicide based alloys were calculated using the average measured compositions of the Nb_{ss}, the equations 1 to 5, the equation for Q and data from [72, 64] and are given in Table 1. In the latter the actual average composition of each of the fifty four Nb_{ss} of this study is given and the type of the Nb_{ss} is identified as normal when the Nb_{ss} contains Si, as Nb_{ss} rich in Ti (when the concentration of Ti was high in the Nb_{ss} and the latter exhibited different contrast under back scatter imaging conditions in the SEM and in EPMA [2 – 4, 6, 8 – 10, 29, 67 - 70]) and as Nb_{ss} with no Si (when no Si was detected in the Nb_{ss} using EPMA [e.g., 4, 5]). The Nb_{ss} rich in Ti was present only in alloys in the as cast condition and the Nb_{ss} with no Si was mostly found in alloys in the heat treated condition. The formation of Si free Nb_{ss} is important because this type of solid solution is expected to have enhanced toughness and ductility. The Ti content of the Nb_{ss} is also important because of the effect of sd and sp electronic configuration elements (the concentrations of which depend on the solubility of Ti in the Nb_{ss} [29, 67]) on the mechanical properties and oxidation of the solid solution [6]. The values of the above six parameters for the different types of bcc Nb solid solution are summarised in Table 2.

Mundy et al [75] attributed the diffusion behaviour of W in Nb solid solution alloys to changes in electronic and atomic structure in the solid solution. Ebrahimi and Riuz-Aparicio [76] reported that diffusivity in the bcc solid solution β phase in Nb-Ti-Al alloys was composition dependent and that the diffusivity of Ti was essentially the same at that of Al, owing to the strong bonding between Ti and Al atoms. Ariel Perez et al [77] showed that the diffusivity of solutes in Ti and Zr at 1373 K decreases with atomic size. A similar trend was shown by Hahn and Averback [78] for the diffusion of impurities (Au, Bi, Co, Cr, Cu, Fe, Ti) in amorphous Ni-Zr at 573 K, who also reported strong dependence of atomic mobility on atomic size and rapid decrease of mobility with increasing atomic radius.

The available data [79-87] for the atomic size, Pauling electronegativity, activation energy for diffusion and diffusivity of different solutes in Nb at 1473 K are plotted in figures 1 to 4. In these figures the sd solutes Cr, Fe, Hf, Mo, Ta, Ti, V, W are grouped together depending on their position in the Periodic Table and the sp solutes Al, B and Sn are shown in green. Nb is a group 5 element. Atomic size drops as group number increases. Trends in Pauling electronegativity are nearly opposite to atomic volume. In figures 1 and 2 the trends for the sd solutes in groups higher than group 5 (plus V) are shown in blue dashed lines and the trends for the sd elements in groups 4 and 5 (excluding V) are shown in red dashed lines. In the figures 3 and 4 the trends for the sd solutes in groups higher than group 5 are shown in blue dashed lines and the trends for the sd elements in groups 4 and 5 are shown in red dashed lines. In figures 1 and 2 the data for B is in the trend of the data for the sd elements in groups higher than group 5 but in figures 3 and 4 is in the trend of the data for the sd elements in the groups 4 and 5. In figures 1 and 2 the data for Al and Sn is in the trend of the data for the sd elements in groups 4 and 5 but in figures 3 and 4 is in the trend of the data for sd elements of groups higher than group 5. In other words the atomic size and electronegativity allow one to differentiate the diffusion of Al, B and Sn in bcc Nb_{ss}. These three solute elements are very important for the oxidation of Nb silicide based alloys.

The data in figures 1 and 2 show that the diffusion coefficients at 1473 K and the activation energy for diffusion of sd solutes in Nb that are on the right hand side of Nb respectively decrease and increase with increasing atomic size and that the diffusivity and activation energy respectively increase and decrease for sd solutes that are on the left of groups 4 and 5 in the Periodic Table and the sp elements Al and Sn.

The same trend as in figure 1 is shown in figure 3 for the activation energy of diffusion with increasing Pauling electronegativity of sd solutes on the right and left of Nb in the Periodic Table but not for the simple metals Al, B and Sn.

It is well known from the violation of Vegard's rule that the size of a solute atom is an ambiguous parameter because it depends on the environment in which the solute atom finds itself in an alloy and is different when the same solute is in different alloys [88] owing to electronic interactions [89]. Data for the effective atomic size of solute atoms in Nb_{ss} is not available, thus in this work the atomic size data for elements was used to calculate the parameter δ.

The reduction of effective atomic size due to the charge transfer enables solute atoms much smaller than the solvent atoms to diffuse as interstitials, meaning that such solutes can have a faster than the expected diffusivity compared with solutes with size difference less than the Hume-Rothery limit of $\pm$ 15% [90]. Elastic interaction and therefore the elastic strains the solute exerts on its surrounding due to the difference in size (size misfit) is also important. The case where the elastic interaction dominates was considered by Zener [91] who showed that the activation energy is proportional to $\mu\varepsilon_o^2$ where the elastic modulus of the solvent is μ and ε_o is strain in the surroundings of the solute atom when the latter is at the saddle point. The bigger the size of the diffusing solute the greater the migration energy should be due to the increased work to push the atom through a gate of surrounding atoms. At the same time the vacancy formation energy is decreased in the compressive strain field of a solute atom bigger than the solvent which leads to a binding energy between solute and vacancy and thus a decrease in the activation energy of diffusion. The latter however is small, and therefore with solute atoms larger than the solvent an increase in activation energy of diffusion and a corresponding decrease in diffusivity is expected.

Are there any trends (correlations) between the studied parameters of the fifty four Nb solid solutions and more specifically with the parameters δ and $\Delta\chi$ that depend respectively on atomic size and electronegativity? To answer this question the data in Table 1 was used to identify trends between the six parameters. Figures 5 to 7 are selected typical examples and will be discussed below. No trends were found between ΔH_{mix} and ΔS_{mix}, VEC and ΔS_{mix}, VEC and ΔH_{mix}, and Q and VEC (figures not shown).

In the figures 5 to 7 the part (a) includes the data for all the solid solutions in Table 1. In all the parts (a) of the figures 5 to 7 the series 2 data is for Nb_{ss} in alloys with RM, TM, and Sn but no Al, the series 3 data is for Nb_{ss} in alloys with RM, TM, Ge and Sn and with/out Al and Cr, the series 4 data is for Nb_{ss} in alloys with TM, Al, with/out Hf, no RM and no B, Ge, Sn, the series 5 data is for Nb_{ss} in alloys with TM, Al and B, with/out Hf, the series 6 data is for Nb_{ss} in alloys with TM, Al and with/out B, Ge, Hf and Sn, the series 7 data is for Nb_{ss} in alloys with RM, TM with/out Al and with no B, Ge, Sn and the series 8 data is for Nb_{ss} in alloys with TM, Al with/out RM, B or Sn and no Ge. The part (b) of each figure shows the data for Nb_{ss}

with no Si and Nb_{ss} rich in Ti from Table 1. In each part (b) of the figures 5 to 7 the series 2 data is for the Nb_{ss} rich in Ti and the series 3 is for the Nb_{ss} with no Si.

Figure 5 shows that high values of δ are linked with more negative ΔH_{mix}. A similar correlation between the same parameters has been reported for solid solution phases and amorphous alloys [58, 92 - 94]. The latter tend to have higher δ and more negative ΔH_{mix}. In Figure 5(a) the "basis" bcc Nb_{ss} i.e., the solid solution with Al, Cr, Si, Ti and Hf solutes or $(Nb,Al,Cr,Hf,Si,Ti)_{ss}$ (the term "basis" Nb_{ss} is used through-out the paper to describe the aforementioned bcc Nb_{ss} solid solution) occupies the centre of the figure (series 4), alloying with B (series 5) "pushes" the Nb_{ss} to the high δ and the most negative ΔH_{mix} values, while alloying with RMs with no B, Ge and Sn addition(s) "places" the Nb_{ss} in the area of low δ and less negative ΔH_{mix} values (series 7). Series 3 in Figure 5(b) shows that alloying with RMs and the synergy of the latter with Sn and Ge encourages the formation of the Nb_{ss} with no Si (see also series 7 and the majority of the series 3 data in figure 5(a)) while alloying with Ge, promotes the Nb_{ss} rich in Ti (series 2 in figure 5(b)). Series 2 and 3 in figure 5(b) are separated at $\delta \approx 5$ (vertical dotted line). Similar separation at $\delta \approx 5$ was found in ΔS_{mix} versus δ, VEC versus δ and Q versus δ diagrams (not shown). The Nb_{ss} with no Si contains no B and no Ta, is rich in the refractory metals Mo and W with Mo + W > 15 at%, Mo/W < 3 and Ti/(Mo + W) < 1. The Ti rich Nb_{ss} can contain B and the refractory metals Mo, Ta and W but is poor in Mo + W (< 10 at%) and has Mo/W > 3 and Ti/(Mo + W) > 2.

Figure 6 shows the data for $\Delta\chi$ and ΔH_{mix}. In both parts of this figure the data falls in two groups that are indicated by ellipses. For the studied solid solutions $\Delta\chi$ values were not found in the range 0.13 to 0.179. The solid solutions with $\Delta\chi > 0.179$ have no B, Ta and V and the solid solutions with no W have $\Delta\chi < 0.13$. In Figure 6(a) the "basis" Nb_{ss} (series 4) is in the bottom ellipse together with the series 5, 6 and 8 data. In this ellipse, upon alloying the "basis" Nb_{ss} with the elements B, Ge, Sn, RM and TM there is a shift towards more negative ΔH_{mix} values. The Nb_{ss} with solutes only RMs and no B, Ge, Sn (series 7), or RMs and Sn and no Al (series 2) and RMs and Ge and Sn (series 3) belongs to the top ellipse. In the latter, the Nb_{ss} with RMs and no B, Ge, Sn (series 7) has $0.23 < \Delta\chi < 0.26$ but when the solid solution contains RMs with Sn or with Ge and Sn the ranges of $\Delta\chi$ and ΔH_{mix} values increase. In figure 6(b) the bottom ellipse has Ti rich Nb_{ss} with no RMs. Ti rich Nb_{ss} with RMs belongs in the bottom of the top ellipse. These solid solutions are lean in Mo and W and have Mo + W < 10 at%, Mo/W > 3 and Ti/(Mo + W) > 2. In figure 6(b) the Nb_{ss} with no Si (series 3) has $0.23 < \Delta\chi \leq 0.33$ and ΔH_{mix} less negative than - 9.5 $kJmol^{-1}$ and the Nb_{ss} rich in Ti with RMs (series 2) has lower $\Delta\chi$ and more negative ΔH_{mix} values. Gap in $\Delta\chi$ values was also exhibited in diagrams of $\Delta\chi$ versus Q, $\Delta\chi$ versus VEC, $\Delta\chi$ versus ΔS_{mix} and $\Delta\chi$ versus δ (figures not shown).

Figure 7 shows that higher values of Q correspond to less negative ΔH_{mix} and is included in this paper to demonstrate that trends between other parameters (in this case Q and ΔH_{mix}) do not allow one to differentiate between different types of solid solution and thus to further highlight the importance of the parameters δ and $\Delta\chi$.

Partitioning describes the redistribution of a solute between the phases that take part in a transformation. The redistribution of solute involves diffusion. The formation of Nb solid

solution in Nb silicide based alloys is accompanied by the partitioning of solutes between the phases (solid solution(s) and intermetallic(s)) [29, 67], and therefore diffusion of solutes plays an important role in defining the composition of the solid solution(s) and the type(s) of Nb_{ss} that is(are) observed in the microstructure. In Nb silicide based alloys Mo and W partition strongly to the Nb_{ss} rather than the 5-3 silicide but Ti partitions to both phases. In the solid solution Mo and W have opposite partitioning behaviour compared with Ti, meaning the concentrations of Mo and W in the Nb_{ss} decrease with increasing Ti content. The concentration of B in the solid solution decreases with increasing Ti concentration but the concentrations of Cr, Hf and Sn in the Nb_{ss} increase with that of Ti. The case of Al is more complicated and depends on which elements are present in the alloy, meaning the Al concentration can increase or decrease with increasing Ti concentration. In other words Cr, Hf and Sn follow ("like") Ti but B, Mo and W do not and Al "chooses" how to behave.

Figures 1 to 4 show that the aforementioned elements belong in different groups regarding their activation energy for diffusion and diffusivity at 1473 K. They also show that electronegativity and atomic size can differentiate the behaviour of the sp elements. The Nb_{ss} with no Si is formed when the solid solutions are rich in Mo and W but not when Ta is present in the alloy [67]. We can understand this if we consider the contrasting sequences of atomic volumes ($Å^3$/atom) [Ta (18.1) > Nb (18.05) > W (15.82) > Mo (15.61)] and Pauling electronegativity [Ta (1.5) < Nb (1.6) < Mo (2.16) < W (2.36)] which suggest strong binding between Nb-Mo and Nb-W and weaker binding between Nb-Ta. The formation of Ti rich Nb_{ss} and Nb_{ss} with no Si is attributed to the partitioning of Mo, Ti and W.

With the exception of the 79.7Nb-10.3Mo-7.9W-2.1Hf bcc Nb solid solution in Table 1, the other fifty three solid solutions have between five and ten elements. None of the solid solutions in Table 1 satisfies the standard definition of a high entropy alloy (HEA) as "an alloy that contains at least five major metallic elements, each having concentrations between 5 to 35 at%" [95]. Comparison of the data in Tables 1 and 2 with data reported for solid solution phase high entropy alloys (HEAs) and the reported ranges of the values of the same six parameters for the formation of solid solution phase HEAs [58, 62, 64, 92 - 94, 96, 97] shows that parameters of some of the solid solutions in Nb silicide based alloys are in the ranges proposed for solid solution phase HEAs. In Table 1 the values of parameters that are outside the ranges reported for solid solution HEAs are given in bold numbers. There are differences for the parameters $\Delta\chi$, δ and ΔS_{mix}. These are discussed below.

Young et al [93] reported that solid solution phase HEAs have $0.10 < \Delta\chi < 0.15$, that HEAs containing intermetallics or mixture of solid solution and intermetallics have $0.15 < \Delta\chi < 0.25$ and that the value $\Delta\chi = 0.175$ separates solid solution phases and intermetallics. The $\Delta\chi$ values of the three types of bcc Nb_{ss} of this study fall in the wider range 0.039 to 0.331, but specific bcc Nb_{ss} solid solution types have different ranges (Table 2). The solid solutions with $\Delta\chi > 0.179$ have no B, Ta and V and the solid solutions with no W have $\Delta\chi < 0.13$. It is interesting to notice that in the electronegativity based figures 3 and 4 the former three elements belong in the same group (red dashed lines). Table 2 and figure 6 show that there is a gap in $\Delta\chi$ values of the fifty four Nb_{ss} studied in this paper and would suggest that no bcc Nb solid solution forms with $\Delta\chi$ values in the range $0.13 < \Delta\chi < 0.179$. Research is needed to clarify this point.

According to the literature (i) solid solution phases in HEAs form when the parameters δ, ΔH_{mix} and ΔS_{mix} respectively are in the ranges $0 \leq \delta \leq 8.5$, $-22 \leq \Delta H \leq 7$ kJmol^{-1} and $11 \leq \Delta S \leq 19.5$ Jmol^{-1}K^{-1} and (ii) by decreasing δ to less than 4 while keeping ΔH_{mix} and ΔS_{mix} in the above ranges only solid solution would form and no intermetallics [64]. The enthalpy values from the Miedema model are not accurate, and reliable enthalpy data from DFT and CALPHAD modelling is needed. Standard and operational definitions of HEAs have been discussed by Miracle et al [98]. There is no unanimous agreement about what the ΔS_{mix} value should be. For example in reference [64] it is suggested that for HEAs $\Delta S_{mix} > 11$ Jmol^{-1}K^{-1}, while the data in reference [96] suggests $\Delta S_{mix} > 11.5$ Jmol^{-1}K^{-1}. Miracle and co-workers [98] considered $\Delta S_{mix} \geq 1.5R$ (12.47 Jmol^{-1}K^{-1}) as an operational definition of an HEA. The entropy of mixing values that satisfy the aforementioned definition are shown by italic numbers in Table 1 while those that are less than 11 Jmol^{-1}K^{-1} are shown by bold numbers. Only seven bcc Nb_{ss} solid solutions in Table 1 (four Nb_{ss} with no Si, two Nb_{ss} Ti rich and one normal Nb_{ss}) with eight or more elements have $\Delta S_{mix} \geq 1.5R$.

The data in Table 2 shows that the parameter δ for the normal and Ti rich bcc Nb_{ss} solid solutions exceeds the upper limit of δ of the HEAs. It should be noted that Yang and Zhang [97] suggested a lower upper limit of δ (< 6.6) for formation of solid solution phases in HEA. The highest value of the parameter δ for the bcc Nb_{ss} with no Si is smaller than 6.6 (Table 2).

In the literature [62, 93] values of the parameter VEC are given for bcc (< 6.87) and fcc (> 7.8) solid solution phase HEAs and for mixture of bcc and fcc solid solution phase (6.87 < VEC < 7.8) HEAs, which is consistent with the trend of VEC of metals in the Periodic Table. Comparison with the data in Table 2 shows that all three types of bcc Nb_{ss} solid solution that can form in Nb silicide based alloys have VEC in the range reported for bcc solid solution phase HEAs**.**

Yang and Zhang [97] suggested that solid solution phase HEAs should have Q > 1.1. All types of bcc Nb_{ss} solid solutions of this study had Q values higher than 1.1 (Tables 1 and 2).

The data for the different types of bcc solid solution in Table 2 and corresponding data for the Nb silicide based alloys (Part II [66]) can be used to design alloys to meet property goals. This will be the subject of a separate publication.

Conclusions

Three types of bcc Nb_{ss} solid solution can form in Nb silicide based alloys, namely the normal Nb_{ss}, Ti rich Nb_{ss} and Nb_{ss} with no Si. Using data for the chemical composition of fifty four solid solutions in alloys studied previously, the parameters ΔH_{mix}, ΔS_{mix}, VEC, δ, $\Delta\chi$, and Q were calculated and their values were found to be in the ranges $-2 < \Delta H_{mix} < -15.9$ kJ/mol, $5.8 < \Delta S_{mix} < 14.5$ J/molK, $2.4 < \delta < 9.7$, $4.4 <$ VEC < 5.4, $0.039 < \Delta\chi < 0.13$ and $0.179 < \Delta\chi < 0.0331$ and $1.55 < Q < 8.9$. The solid solutions with $\Delta\chi > 0.179$ had no B, Ta and V and the solid solutions with no W had $\Delta\chi < 0.13$. The atomic size difference parameter δ could separate the Nb_{ss} rich in Ti ($\delta > 5$) and the Nb_{ss} with no Si ($\delta < 5$).

Acknowledgements

Helpful discussions with Drs K Zelenitsas, J Geng, N Vellios, I Grammenos, T Thandron, E Zacharis, Zifu Li, C Utton, A Tweddle, I Papadimitriou, J Nelson, Z Xu and Mr B Anazodo, Mr G Bywater and Mr C McCaughey and support of the research by the EPSRC, Rolls Royce plc and the University of Sheffield are gratefully acknowledged.

References

1. B P Bewlay, M R Jackson, M F X Gigliotti. in Intermetallic Compounds: Principles and Practice, Volume 3, R L Fleischer and J H Westbrook, eds, John Wiley, New York, NY, 2001; p541

2. N Vellios and P Tsakiropoulos, Intermetallics 18 (2010) 1729-1736

3. Zifu Li and P Tsakiropoulos, Intermetallics 26 (2012) 18-25

4. I Grammenos and P Tsakiropoulos, Intermetallics 19 (2011) 1612-1621

5. I Grammenos and P Tsakiropoulos, Intermetallics 18 (2010) 1524-1530

6. J Geng and P Tsakiropoulos, Intermetallics 15 (2007) 382-395

7. M G Mendiratta and D M Dimiduk, Scripta Met. Mater. 25 (1991) 237-242

8. T Thandron and P Tsakiropoulos, Intermetallics 18 (2010) 1033-1038

9. Zifu Li and P Tsakiropoulos, Intermetallics 19 (2011) 1291-1297

10. Zifu Li and P Tsakiropoulos, Journal Alloys Compounds 550 (2013) 553-560

11. V P Bondarenko, L A Dvorina, N P Slyusar and E N Fomichev, Poroshkovaya Metallurgiya, number 11 (107) (1971) 48-51

12. S V Meschel and O J Kleppa, Journal Alloys and Compounds 274 (1998) 193-200

13. P B Fernandes, G C Coelhoa, F Ferreira, C A Nunes and B Sundman, Intermetallics 10 (2002) 993-999

14. M E Schlesinger, A B Gokhale and R Abbaschian, J. Phase Equil. 14 (1993) 502-509

15. P R Subramanian, M G Mendiratt and D M Dimiduk, Mater. Res. Soc. Symp. Proc. vol.322 (1994) 491-502

16. H Liang andY A Chang, Intermetallics 7 (1999) 561-570

17. Y Yang, Y A Chang, J C Zhao and B P Bewlay, Intermetallics 11 (2003) 407-415

18. E Fitzer and F K Schmid, Monatsh Chem. 102 (1971) 1608-1625

19. N David, Y Cartigny, T Belmonte, J M Fiorani and M Vilasi, Intermetallics 14 (2006) 464-473

20. H J Goldschmidt and J A Brand, J. Less Common Met. 3 (1961) 34-43

21. J C Zhao, M R Jackson and L A Peluso, Acta Mater. 51 (2003) 6395-6405

22. J Geng, G Shao and P Tsakiropoulos, Intermetallics 14 (2006) 832-837

23. B P Bewlay, Y Yang, R L Casey, M R Jackson and Y A Chang, Intermetallics 17 (2009) 120-127

24. T Geng, C Li, J Bao, X Zhao, Z Du and C Guo, Intermetallics 17 (2009) 343-357

25. Y Li, C Li, Z Du, C Guo and X Zhao, Rare Metals 32 (2013) 502–511

26. I Papadimitriou, C Utton and P Tsakiropoulos, in preparation

27. I Papadimitriou, C Utton and P Tsakiropoulos, Metal. Mat. Trans. A 46 (2015) 5526-5536

28. M R Jackson, B P Bewaly and J C Zhao, US patent 6,913,655 B2, July 5, 2005

29. K Zelenitsas and P Tsakiropoulos, Intermetallics 13 (2005) 1079-1095

30. K S Chan, Mater. Sci. Eng. A409 (2005) 257-269

31. K S Chan, Mater. Sci. Eng. A337 (2002) 59-66

32. G Ghosh, G B Olson, Acta mater. 55 (2007) 3281-3303

33. W Hume-Rothery, G W Mabbott, K M Channel-Evans, The freezing points, melting points and solid solubility limits of the alloys of silver and copper with the elements of the B sub-groups, Phil. Trans. Royal Soc. London, Series A, 233 (1934), 1-97

34. W Hume-Rothery, R E Smallman, C W Haworth, Structure of Metals and Alloys, Institute of Metals, London, 1969

35. L S Darken, W R Gurry, Physical Chemistry of Metals, McGraw-Hill, New York, 1953

36. K A Cschneidner Jr, Rare Earth Alloys, D. van Nostrand, Princeton, NJ, 1961

37. J T Waber, K A Cschneidner Jr, A C Larson, M Y Prince, Trans. Metall. Soc. AIME, 227 (1963) 717-723

38. J R Chelikowsky, Phys. Rev. B. 19 (1979) 686-701

39. J A Alonso, S Simozar, Phys. Rev. B. 22 (1980) 5583-5589

40. J A Alonso, L M Lopez, S Simozar, Girifalco, Acta metal. 30 (1982) 105-107.

41. L H Bennett, ed., Theory of alloy phase formation, The Metallurgical Society of AIME, Warrendale, PA, 1980

42. T B Massalski, Structure and stability of alloys, in Physical Metallurgy, eds R W Cahn, P Haasen, North Holland, New York, 1996, pp. 135-204

43. A Cottrell, Concepts in the electron theory of alloys, IOM Communications, London, 1998

44. D G Pettifor, William Hume-Rothery: His life and science, in Science of alloys for the 21st century, eds E A Turchi, R D Shull, A Gonis, TMS, Warrendale, PA, 2000, pp. 9-32

45. K A Cschneidner Jr, M Verkade, Progress in Materials Science 49 (2004) 411-428

46. A R Miedema, J. Less Common Met. 32 (1973) 117-136

47. A R Miedema, F R de Boer, P F Dechatel, J. Phys. F. 3 (1973) 1558-1576

48. A R Miedema, R Boom, F R de Boer, J. Less Common Met. 41 (1975) 283-298

49. Van S Blackwood, T W Koenig, J M Porter, D L Olson, B Mishra, R D Mariani, D L Porter, Elemental solubility tendency for the phases of uranium by classical models used to predict alloy behaviour, in Energy Technology 2012: Carbon dioxide management and other technologies, eds MD Salazar-Villalpando et al., John Wiley and Sons Ltd, Hoboken, NJ, DOI:10.1002/9781118365038.ch42

50. O N Senkov, G B Wilks, D B Miracle, C P Chuang, P K Liaw, Intermetallics 18 (2010) 1758-1765

51. D B Miracle, Mater. Sci. Techn. 31 (2015) 1142-1147

52. F Otto, Y Yang, H Bei, E P George, Acta mater. 61 (2013) 2628-2638

53. O N Senkov, J M Scott, S V Senkova, D B Miracle, C F Woodward, J. Alloys Comp. 509 (2011) 6043-6048

54. S Singh, N Wanderka, B S Murty, U Glatzel, J Banhart, Acta mater. 59 (2011) 182-190

55. B Zhang, M C Gao, Y Zhang, S Yang, S M Guo, Mater. Sci. Techn. 31 (2015) 1207-1213

56. A R Miedema, F R de Boer, R Broom, Calphad 1 (1977) 341-359

57. M C Gao, D E Alman, Entropy 15 (2013) 4504-4519

58. Y Zhang, Y J Zhou, J P Lin, G L Chen, P K Liaw, Adv. Eng. Mater. 10 (2008) 534-538

59. I A Tomilin, S D Kaloshkin, Mater. Sci. Techn. 31 (2015) 1231-1234

60. I Papadimitriou, C Utton, A Scott, P Tsakiropoulos, Intermetallics 54 (2014) 125-132

61. I Papadimitriou, C Utton, P Tsakiropoulos, Computational Materials Science 107 (2015) 116-121

62. S Guo, C Ng, J Lu, C T Liu, J Appl. Phys. 109 (2011) 103505

63. A Inoue, Acta mater. 48 (2000) 279-306

64. S Guo, C T Liu, Prog. Nat. Sci. Mater. Intern. 21 (2011) 433-446.

65. O N Senkov, D B Miracle, Mater. Res. Bull. 36 (2011) 2183-2198

66. P Tsakiropoulos, Journal Alloys Compounds, submitted

67. K Zelenitsas, P Tsakiropoulos, Intermetallics 14 (2006) 639-659

68. I Grammenos, P Tsakiropoulos, Intermetallics 18 (2010) 242-253

69. N Vellios, P Tsakiropoulos, Intermetallics 15 (2007) 1518-1528

70. N Vellios, P Tsakiropoulos, Intermetallics 15 (2007) 1529-1537

71. B P Bewlay, R J Grylls, H L Fraser, Mat. Res. Soc. Symp. Proc. Vol. 552 (1999) KK5.27.1-KK5.27.5

72. A Takeuchi, A Inoue, Materials Transactions 46 (2005) 2817−2829.

73. U Mizutani, Hume-Rothery Rules for Structurally Complex Alloy Phases, CRS Press, Boca Raton, FL, 2011

74. U Mizutani, R Asahi, H Sato, T Noritake, T Takeuchi, J Physics: Condens. Matter 20 (2008) 275228

75. J N Mundy, S T Ockers, L C Smedskjaer, Phys. Rev. B, 33 (1986) 847-853

76. F Ebrahimi, J G L Ruiz-Aparicio, Journal Alloys and Compounds 245 (1996) 1-9

77. Rodolfo Ariel Perez, Hideo Nakajima, Fanny Dyment, Materials Transactions 44 (2003) 2-13

78. H Hahn, R S Averback, Phys. Rev. B, 37 (1988) 6533-6535

79. Yajun Liu, Zhaohui Long, Yong Du, Guang Sheng, Jiang Wang, Lijun Zhang, CALPHAD 36 (2012), 110-117

80. Yajun Liu, Tongyan Pan, Lijun Zhang, Di Yu, Yang Ge, Journal of Alloys and Compounds 476 (2009) 429–435

81. Yajun Liu, Guan Wang, Jiang Wang, Zhitao Kang, Journal of Alloys and Compounds 555 (2013) 381–389

82. F Giithoff, B Hemion, C Herzig. W Petry, H R Schober and J Trampenau, J. Phys. Condens. Matter *6* (1994) 6211-6220

83. J A Wheeler Jr, F R Winslow, eds, Diffusion in body-centred cubic metals, ASM, Metals Park, Ohio, 1965

84. I Kaur, W Gust, L Kosma, eds, Handbook of grain and interphase boundary diffusion data, Volume 2, Ziegler Press, 1989

85. N L Peterson, Diffusion in Refractory Metals, Wadd Technical report 60-793, May 1961

86. X. M. Li and Y. T. Chou, Acta mater. 44 (1996) 3535-3541

87. F Roux, A Vignes, Pevue de Physique Applique 5 (1970) 393-405

88. G Shao, P Tsakiropoulos, Mater. Sci. Eng. A, A271 (1999) 286-290

89. S Diplas, G Shao, S A Morton, P Tsakiropoulos, J F Watts, Intermetallics 7 (1999) 937-946

90. H Bakker, J. Less Common Metals, 105 (1985) 129-138]

91. C Zener, Imperfections in Nearly Perfect Crystals, Wiley, New York, 1950

92. S Guo, Q Hu, C Ng, C T Liu, Intermetallics 41 (2013) 96-102

93. X Yang, S Y Chen, J D Cotton, Y Zhang, JOM 66 (2014) 2009-2020

94. W H Liu, Y Wu, J Y He, Y Zhang, C T Liu, JOM 66 (2014) 1973-1983

95. J-W Yeh, Ann. Chim. Sci. Mater. 31 (2006) 633-648

96. O N Senkov, C Woodward, D B Miracle, JOM 66 (2014) 2030-2042

97. X Yang, Y Zhang, Mater. Chem. Phys. 132 (2012) 233-238

98. D B Miracle, J D Miller, O N Senkov, C Woodward, M D Uchic, J Tiley, Entropy 16 (2014) 494-525.

Table 1: The values of the parameters ΔH_{mix} (kJmol^{-1}), ΔS_{mix} (Jmol^{-1}K), VEC, δ, $\Delta\chi$, T_m (K) and Q of different types of bcc Nb_{ss} formed in Nb silicide based alloys (for **bold numbers** and *numbers in italics* see text)

bcc Nb_{ss} (at%)	**Condition***	**Nb_{ss} type**	**Parameter**						
			ΔH_{mix}	ΔS_{mix}	VEC	δ	$\Delta\chi$	Tm	Q
55.3Nb-12.7Ti-1.8Si-1.1Hf-10.7Mo-7.5W-2Sn-8.8Cr	AC	normal	-7.8	11.95	5.09	5.12	**0.260**	2614	4
36.3Nb-33Ti-2.1Si-2.2Hf-4.5Mo-0.9W-7.3Sn-13.6Cr	AC	Ti rich	-8.32	*12.83*	4.74	6.9	**0.179**	2226	3.4
37.4Nb-22.5Ti-4.2Si-2.4Hf-5.1Mo-1.5W-3.8Sn-22.5Cr	AC	Ti rich	-12.58	*13.31*	4.84	7.8	**0.184**	2390	2.44
49.5Nb-18.5Ti-0.5Si-0.9Hf-10.3Mo-5.3W-3.1Sn-12.1Cr	HT	normal	-5.18	12.32	5.06	5.53	**0.312**	2525	6
65.9Nb-12.9Ti-2.1Si-1.3Hf-9.2Mo-4.7W-2.2Sn-1.7Cr	AC	normal	-3.87	**9.92**	4.97	4.1	**0.233**	2619	6.7
57.6Nb-21.3Ti-1.7Si-2.3Hf-7.2Mo-2.3W-3.5Sn-4.1Cr	AC	Ti rich	-4.55	**10.05**	4.85	4.97	**0.203**	2427	5.36
61.2Nb-17.5Ti-0.5Si-1Hf-9.4Mo-3.7W-2.9Sn-3.8Cr	HT	normal	-3.8	**10**	4.95	3.3	**0.224**	2563	6.74
55Nb-22Ti-2.3Si-1.7Hf-11.5Mo-5.3Sn-2.2Cr	AC	normal	-6.8	**10.45**	4.82	8.1	**0.205**	2429	3.73
53.4Nb-23.6Ti-0.3Si-0.6Hf-13.7Mo-3.7Sn-4.7Cr	HT	normal	-3.25	**10.49**	4.91	4.5	**0.210**	2465	7.96
81.7Nb-1.7Si-3.5Hf-8.4Mo-4.7W	AC	normal	-5	**5.8**	5.08	3.56	**0.228**	2780	3.21
78.2Nb-0.4Si-1.8Hf-9.3Mo-10.3W	AC	normal	-5	**6.17**	5.17	2.62	**0.273**	2852	3.52
79.7Nb-0Si-2.1Hf-10.3Mo-7.9W	HT	no Si	-2	**5.8**	4.69	2.4	**0.26**	2835	8.1
71.3Nb-8.8Ti-1.3Si-2.5Hf-10.1Mo-6W	AC	normal	-5.5	**8.35**	5.04	3.34	**0.248**	2730	4.17

71.1Nb-11.5Ti-0.Si-2.7Hf-9.9Mo-4.8W	HT	no Si	-2.44	**8**	5.00	2.7	**0.236**	2710	8.9
64.5Nb-10Ti-0Si-3.4Hf-10Mo-7.2W-4.8Al	AC	no Si	-5.8	**9.92**	4.94	2.8	**0.26**	2609	4.47
63.4Nb-11.7Ti-0Si-2.3Hf-11.1Mo-5.7W-6.1Al	HT	no Si	-6.5	**10**	4.92	2.57	**0.25**	2617	4.04
32.9Nb-7.7Ti-0Si-0Hf-30.2Mo-19.5W-1.8Sn-0.6Ge-3.9Cr-3.4Al	AC	no Si	-6.65	*13.20*	5.06	4	**0.325**	2782	5.52
18.1Nb-11.9Ti-0Si-0Hf-27.1Mo-24W-1.1Sn-1Ge-13.3Cr-3.5Al	HT	no Si	-6.3	*14.5*	5.4	4.9	**0.331**	2742	6.32
65.4Nb-7.2Ti-1.7Si-0Hf-16Mo-7.4W-1.8Sn-0.5Ge	AC	normal	-6.2	**9.3**	5.12	3.9	**0.272**	2306	3.47
69.7Nb-10.1Ti-0Si-0Hf-12Mo-5.2W-2.4Sn-0.6Ge	HT	no Si	-3.42	**8.41**	5.04	3.06	**0.244**	2672	6.57
62Nb-11.4Ti-1.3Si-0.6Hf-12.8Mo-6.2W-4Sn-1.7Ge	AC	normal	-7.51	**10.51**	5	4.48	**0.260**	2389	3.21
54Nb-6.3Ti-0Si-0.2Hf-23.4Mo-13.4W-1.2Sn-1.5Ge	HT	no Si	-4.74	**7.03**	5.28	3.29	**0.313**	2809	4.17
65.5Nb-11.4Ti-1Si-0.3Hf-11.3Mo-4.1W-1.7Sn-0.4Ge-2.1Cr-2.2Al	AC	normal	-6.77	**10.16**	4.98	3.83	**0.235**	2605	3.91
55.2Nb-19.7Ti-1.3Si-1Hf-8.3Mo-1.5W-3.4Sn-0.5Ge-6.2Cr-2.9Al	AC	Ti rich	-7	11.94	4.84	5.06	**0.197**	2429	4.14
64.2Nb-8.6Ti-0Si-0.4Hf-13Mo-5.2W-1.6Sn-0.7Ge-2.4Cr-3.9Al	HT	no Si	-6.526	**10.42**	5.02	5.44	**0.248**	2616	4.18
46Nb-12.9Ti-1Si-0.6Hf-19.3Mo-5.2W-1.6Sn-1Ge-7.8Cr-4.6Al	AC	normal	-9.7	*13.5*	5.06	5	**0.269**	2532	3.52
47.5Nb-9.3Ti-0Si-0.5Hf-21.6Mo-9.9W-1.3Sn-0.9Ge-4.9Cr-4.1Al	AC	no Si	-9.5	*12.8*	4.77	4.17	**0.298**	2653	3.58
48Nb-7.8Ti-0Si-0.1Hf-20.3Mo-9.6W-1.2Sn-0.1Ge-9.4Cr-3.5Al	HT	no Si	-5.86	*12.46*	5.23	4.47	**0.291**	2456	5.22
39.4Nb-16.1Ti-1.5Si-0.9Hf-13.7Mo-3.6W-3.5Sn-1.2Ge-12Cr-8.1Al	AC	normal	-12.2	12.17	4.69	6.04	**0.242**	2343	2.34

50.6Nb-7.7Ti-0Si-0.4Hf-18.2Mo-11.1W-2.1Sn-1Ge-4.7Cr-4.2Al	AC	no Si	-4.56	12.33	4.78	4.22	**0.325**	2642	7.14
44.1Nb-8.2Ti-0Si-0.3Hf-23.5Mo-9.2W-1.3Sn-0.6Ge-9.4Cr-3.4Al	HT	no Si	-7.41	*13.04*	5.25	4.61	**0.295**	2650	4.66
54.3Nb-26.8Ti-2Si-10.7Cr-6.2Al	AC	normal	-10.5	**9.76**	4.69	5.02	0.056	2338	2.17
49.1Nb-32Ti-2Si-10.7Cr-6.2Al	AC	Ti rich	-10.3	**10**	4.64	5.07	0.057	2296	2.23
55.2Nb-24.8Ti-0.3Si-12.2Cr-7.5Al	HT	normal	-7.86	**9.5**	4.72	4.6	0.039	2340	2.83
54Nb-26.5Ti-1.7Si-3.6Hf-8Cr-6.2Al	AC	normal	-9.1	**10.38**	4.64	4.94	0.074	2351	2.68
45.5Nb-30.7Ti-2.3Si-5.6Hf-9.4Cr-6.5Al	AC	Ti rich	-11.05	11.29	4.58	5.6	0.09	2292	2.34
53.8Nb-27Ti-0.5Si-2.2Hf-9.4Cr-7.1Al	HT	normal	-7.5	**10.04**	4.66	4.54	0.059	2338	3.13
35.9Nb-36.4Ti-1.7Si-3.7Hf-4.7Sn-10.9Cr-6.7Al	AC	normal	-11.5	12.42	4.51	6.15	0.112	2139	2.31
52.3Nb-27.9Ti-2.1Si-1.7Ge-9.2Cr-6.8Al	AC	normal	-12.87	**10.38**	4.64	5.12	0.078	2300	1.85
45.4Nb-31.3Ti-1.8Si-1.6Ge-12.9Cr-7Al	AC	Ti rich	-13	**10.9**	4.64	5.52	0.077	2252	1.89
52.6Nb-26.9Ti-0.9Si-1Ge-12.3Cr-6.3Al	HT	normal	-9.7	**10.07**	4.71	5.02	0.062	2323	2.41
48.3Nb-30.6Ti-1.4Si-9Cr-7.4Al-3.3B	AC	normal	-15.91	**10.77**	4.5	**8.95**	0.095	2289	1.55
35.6Nb-39.7Ti-1.3Si-15.7Cr-7Al-0.7B	AC	Ti rich	-11.53	**10.83**	4.59	6.59	0.067	2196	2.06
49.8Nb-28.6Ti-0.5Si-10.7Cr-7.6Al-2.8B	HT	normal	-13.16	**10.53**	4.61	8.37	0.044	2307	1.84
47.5Nb-31.2Ti-1Si-3.2Hf-8.9Cr-5.8Al-2.4B	AC	normal	-12.53	**9.38**	4.57	8.16	0.099	2314	1.73

38.4Nb-36.7Ti-0.9Si-3.5Hf-11.9Cr-5.6Al-3B	AC	Ti rich	-13.61	11.77	4.54	**9.07**	0.104	2254	1.95
51.5Nb-27Ti-0.2Si-2.2Hf-8.5Cr-7.4Al-3.2B	HT	normal	-13.05	**10.84**	4.58	**8.72**	0.098	2329	1.93
27.8Nb-47Ti-0.9Si-4.1Sn-12.1Cr-8.1Al-0B	AC	Ti rich	-9.61	11.15	4.44	5.7	0.091	2031	2.36
40.4Nb-31.5Ti-1.6Si-2.7Hf-1Ge-15Cr-7.8Al	AC	normal	-12.29	11.83	4.63	5.95	0.084	2229	2.15
42.4Nb-27Ti-4.5Si-7.4Ta-11.3Cr-7.4Al	HT	normal	-15.74	12.38	4.65	5.88	0.079	2323	1.83
40.3Nb-31.1Ti-0.6Si-6.8Ta-10.7Cr-6.4Al-4.1B	HT	normal	-15.04	12.38	4.58	**9.69**	0.103	2335	1.92
54.4Nb-26.4Ti-0.6Si-3.2Mo-8.9Cr-6.5Al	HT	normal	-7.58	**10.11**	4.72	4.31	0.109	2366	3.16
45.6Nb-29.8Ti-0.5Si-4.3Mo-11.2Cr-7.6Al-1B	HT	normal	-9	11.37	4.68	6.28	0.130	2304	2.91
55.8Nb-23.6Ti-1.2Si-3.8Hf-2.6Sn-5.2Cr-5.6Al-2.4V	HT	normal	-7.56	11.17	4.64	6.59	0.094	2339	3.46

*AC=as cast, HT=heat treated

Table 2: Ranges of the values of the parameters ΔH_{mix} (kJmol^{-1}), ΔS_{mix} (Jmol^{-1}K^{-1}), VEC, δ, $\Delta\chi^{+}$, T_m (K) and Q of different types of Nb_{ss} formed in Nb silicide based alloys.

Nb_{ss} normal	**Nb_{ss} no Si**	**Nb_{ss} rich in Ti**
$-3.25 < \Delta H_{mix} < -15.91$	$-2 < \Delta H_{mix} < -9.5$	$-4.55 < \Delta H_{mix} < -13.61$
$5.8 < \Delta S_{mix} < 13.5$	$5.8 < \Delta S_{mix} < 14.5$	$10 < \Delta S_{mix} < 13.31$
$4.5 < VEC < 5.17$	$4.69 < VEC < 5.4$	$4.4 < VEC < 4.85$
$2.62 < \delta < 9.69$	$2.4 < \delta < 5.44$	$4.97 < \delta < 9.07$
$0.039 < \Delta\chi < 0.13$ $0.205 < \Delta\chi < 0.312$	$0.236 < \Delta\chi < 0.331$	$0.057 < \Delta\chi < 0.104$ $0.179 < \Delta\chi < 0.203$
$2139 < T_M < 2852$	$2456 < T_M < 2835$	$2031 < T_M < 2429$
$1.55 < Q < 7.96$	$3.58 < Q < 8.9$	$1.89 < Q < 5.36$

+ see text

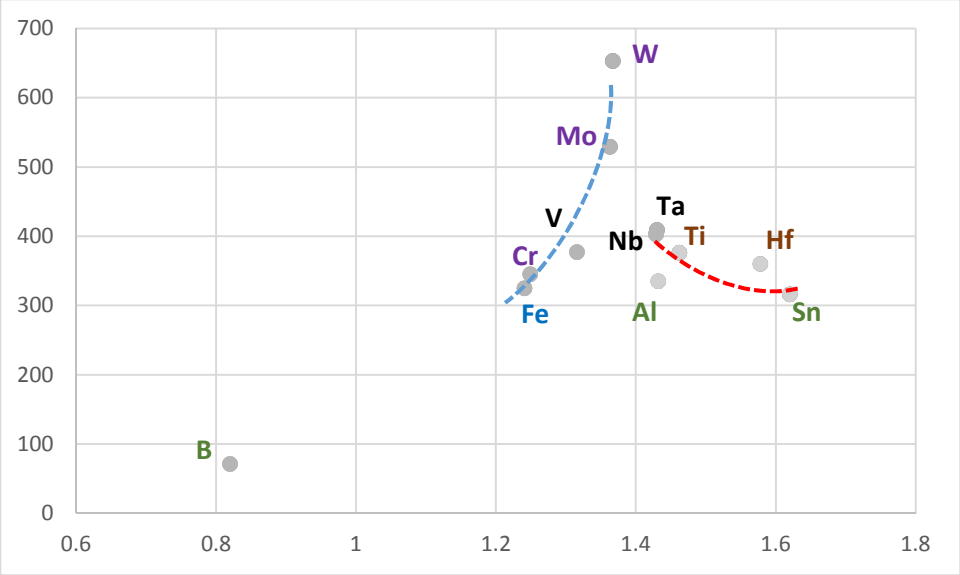

Figure 1 Activation energy (kJ/mol) for diffusion in Nb (ordinate) versus (abscissa) atomic radius (Å) of solutes in Nb

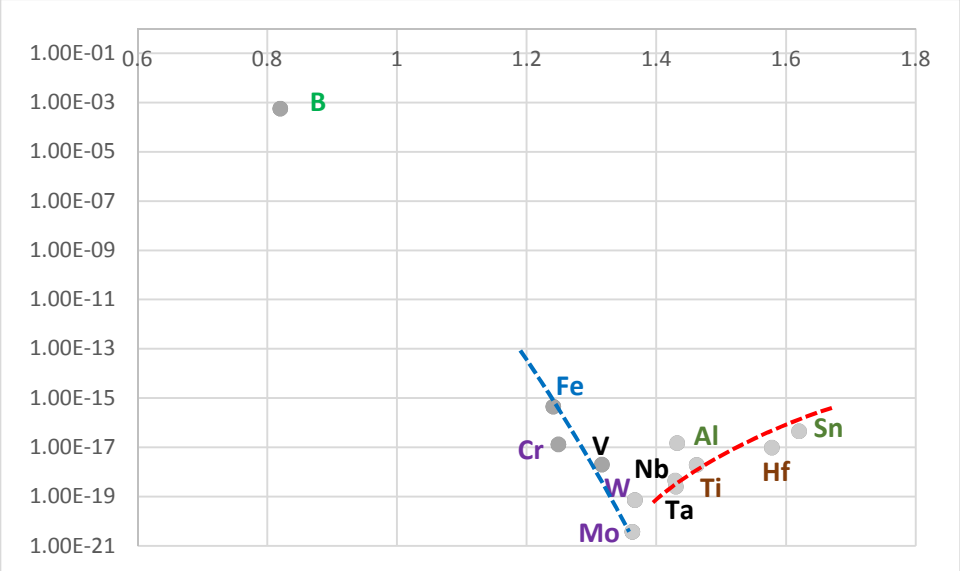

Figure 2 Diffusivity (m^2/s) at 1473 K (ordinate) versus (abscissa) atomic radius (Å) of solutes in Nb

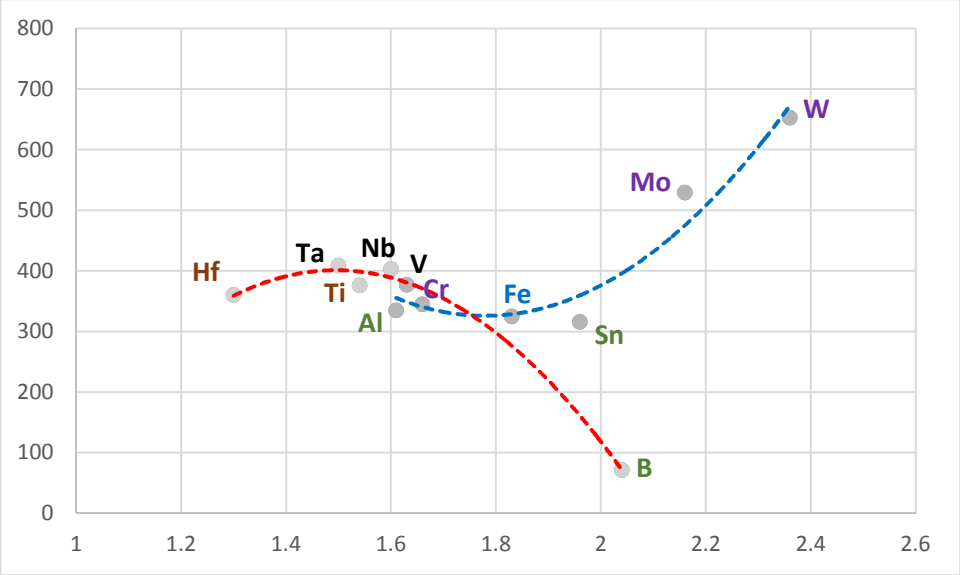

Figure 3 Activation energy (kJ/mol) for diffusion in Nb (ordinate) versus (abscissa) Pauling electronegativity of solutes in Nb

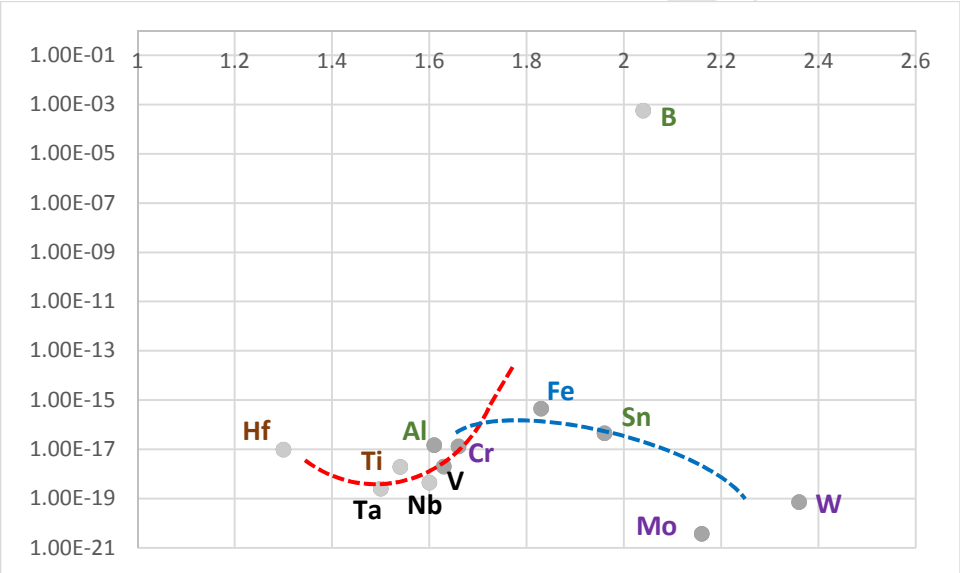

Figure 4 Diffusivity (m^2/s) at 1473 K (ordinate) versus (abscissa) Pauling electronegativity of solutes in Nb

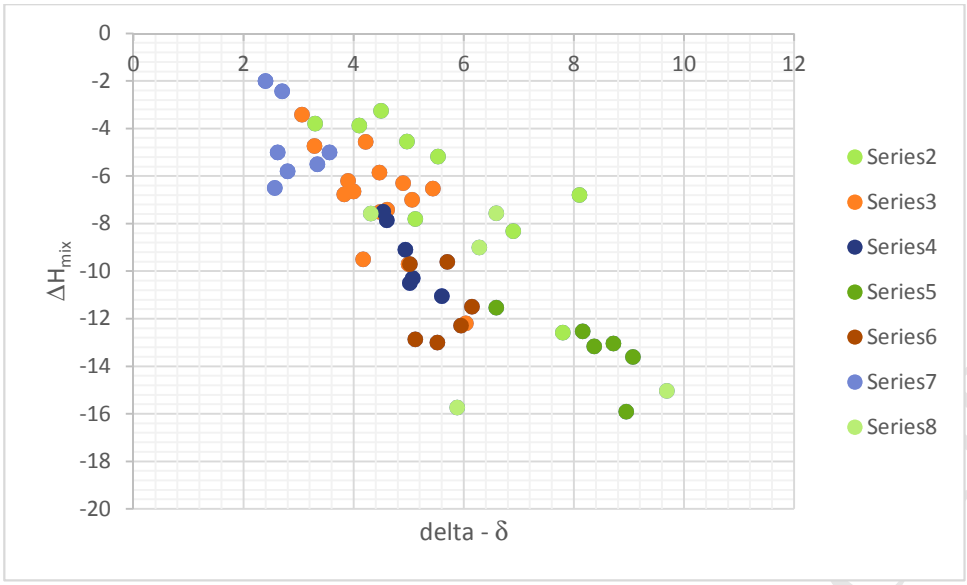

(a)

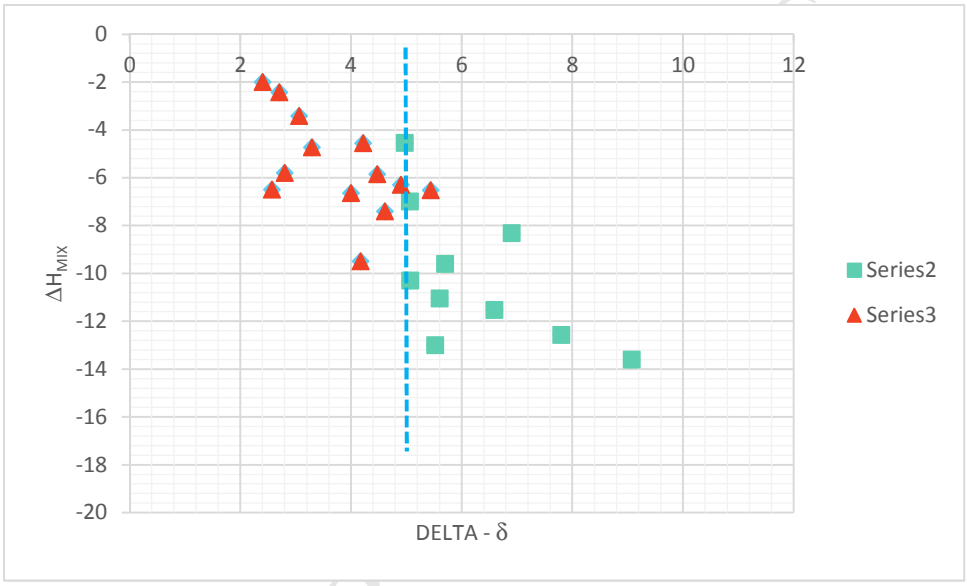

(b)

Figure 5: ΔH_{mix} versus delta (δ) for Nb_{ss}, (a) all data and (b) Nb_{ss} no Si and Nb_{ss} rich in Ti. In (b) series 2 is Nb_{ss} rich in Ti and series 3 is Nb_{ss} with no Si. For dashed line in (b) see text.

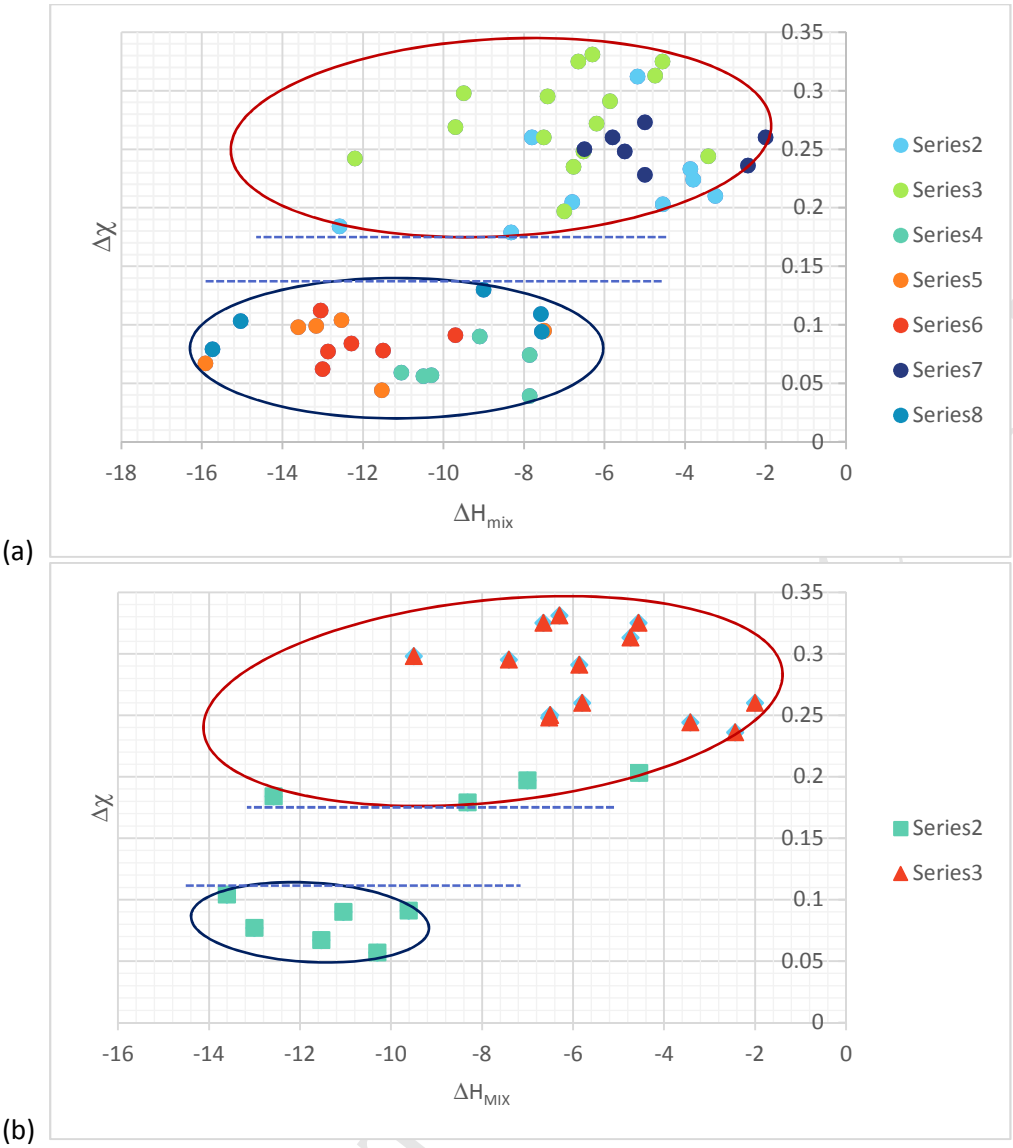

Figure 6: $\Delta\chi$ versus ΔH_{mix} for Nb_{ss}, (a) all data and (b) Nb_{ss} no Si and Nb_{ss} rich in Ti. In (b) series 2 is Nb_{ss} rich in Ti and series 3 is Nb_{ss} with no Si. For dashed lines and ellipses see text.

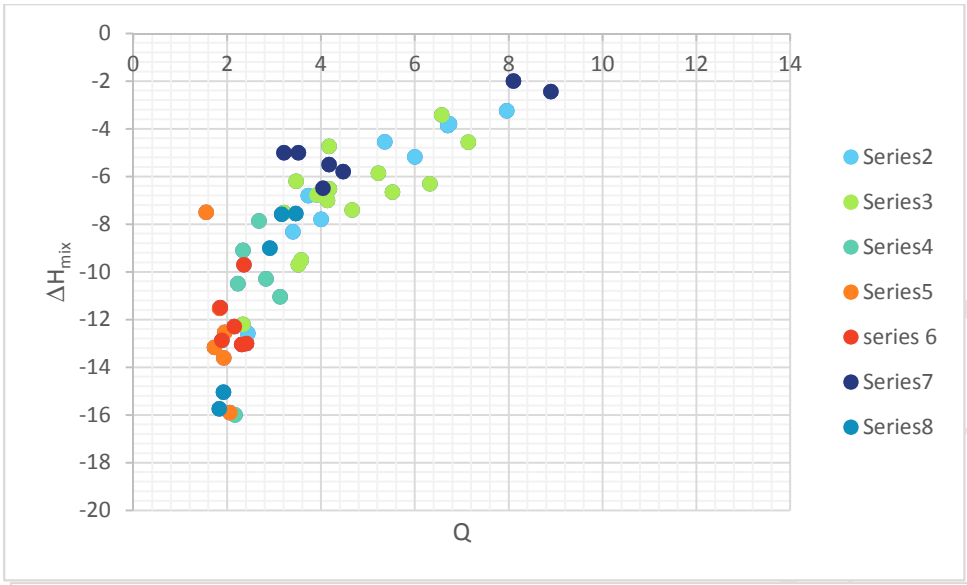

(a)

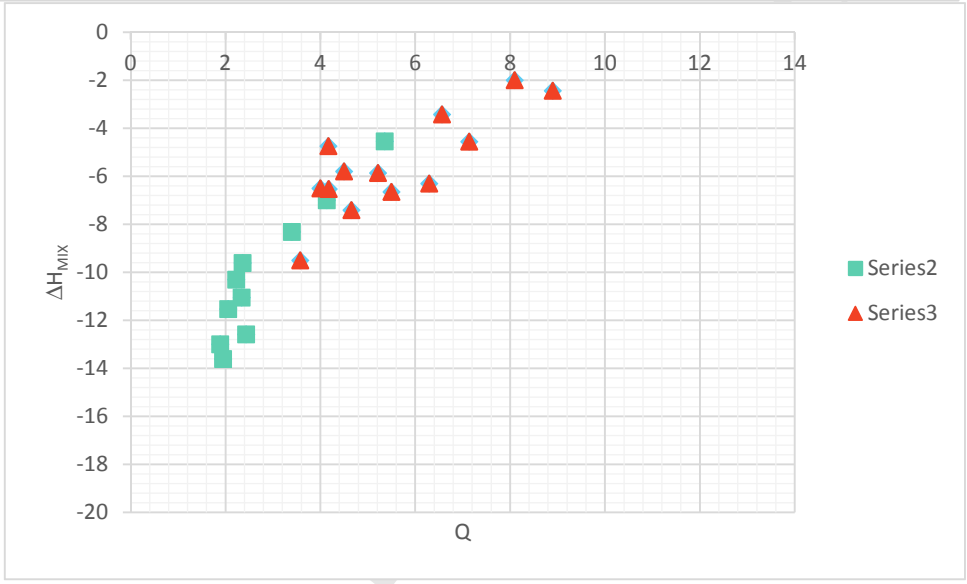

(b)

Figure 7: ΔH_{mix} versus Q for Nb_{ss}, (a) all data and (b) Nb_{ss} no Si and Nb_{ss} rich in Ti. In (b) series 2 is Nb_{ss} rich in Ti and series 3 is Nb_{ss} with no Si.

Highlights

Study of Nb_{ss} using parameters Ω, ΔH_{mix}, ΔS_{mix}, VEC, δ, and $\Delta\chi$

Nb_{ss} with no Si forms has $\delta \leq 5$

$\Delta\chi$ can separate Nb_{ss} with different solute additions